



Wayne State University

---

Wayne State University Theses

---

1-1-2016

# Higher Statistical Uncertainty With Small Pixel Sizes Gives Higher Pass Rates.

Kurt William Van Delinder  
*Wayne State University,*

Follow this and additional works at: [https://digitalcommons.wayne.edu/oa\\_theses](https://digitalcommons.wayne.edu/oa_theses)

 Part of the [Medicine and Health Sciences Commons](#)

---

## Recommended Citation

Van Delinder, Kurt William, "Higher Statistical Uncertainty With Small Pixel Sizes Gives Higher Pass Rates." (2016). *Wayne State University Theses*. 538.  
[https://digitalcommons.wayne.edu/oa\\_theses/538](https://digitalcommons.wayne.edu/oa_theses/538)

This Open Access Thesis is brought to you for free and open access by DigitalCommons@WayneState. It has been accepted for inclusion in Wayne State University Theses by an authorized administrator of DigitalCommons@WayneState.

**HIGHER STATISTICAL UNCERTAINTY WITH SMALL  
PIXEL SIZES GIVES HIGHER GAMMA PASS RATES**

by

**KURT WILLIAM VAN DELINDER**

**THESIS**

Submitted to the Graduate School

of Wayne State University,

Detroit, Michigan

in partial fulfillment of the requirements

for the degree of

**MASTER OF SCIENCE**

2016

MAJOR: MEDICAL PHYSICS

Approved By:

---

Advisor

Date

**© COPYRIGHT BY**  
**KURT WILLIAM VAN DELINDER**  
**2016**  
**All Rights Reserved**

# DEDICATION

*To the pursuit of knowledge and scientific advancement.*

## **ACKNOWLEDGEMENTS**

First and foremost, I would like to thank my advisor, Professor Michael Snyder, Ph.D., for not only designing my excellent research project but, also for dedicating a generous amount of his professional time to working with me on my journey to becoming a master of medical physics. Fulfilling the occupational requirement of a clinical medical physicist, medical physics instructor, researcher and departmental advisor requires an unwavering work ethic and an inattentive view of hours worked within a given week. Regardless, throughout the 1 and 1/3rd years that I have been fortunate enough to work with Mike; he has been able to provide consistent instruction to me, often adapting to my varying work schedule. Being able to have a vocational mentor within arms' reach is a tremendous advantage to an inquisitive student, who desires to reach the pinnacle of their prospective occupation.

Secondly, I would like to thank the department head and chief physicist of the Karmanos Cancer Institute, Jay Burmeister, Ph.D. As the medical physics program director and primary instructor, his creation and overlook over the WSU medical physics educational curriculum has provided me with an exceptionally well-rounded education to allow me to not only fulfill the required tasks of a clinical medical physicist but, also provide me with the necessary tools to become a front-runner for innovation within this technologically advancing field.

Thirdly, I must not forget the WSU department of medical physics additional instructors and also instructional clinical medical physicists. The education process of

becoming a fully certified clinical medical physicist can be likened to working on a large table-based puzzle. The majority of course work will allow you to complete the greater part of the image but it is often the necessary work of the additional educators that allow you to fill in the gaps of the big picture.

Lastly, I would like to thank my classmates for making the two years of rigorous study seem fresh and entertaining. Although, we depart to different tasks, objectives and locations; the field specific meetings bring the members of our occupation together and in short time, we will meet again.

# TABLE OF CONTENTS

DEDICATION.....	ii
ACKNOWLEDGMENTS.....	iii
LIST OF FIGURES.....	vii
<b>Chapter 1 – Introduction.....</b>	<b>(1)</b>
1.1 - Higher Statistical Uncertainty with Small Pixel Sizes Gives Higher Gamma Pass Rates Research Project .....	(1)
1.2 – Radiation Therapy Treatment Planning.....	(2)
1.2.1 – An Introduction to Radiation Therapy Treatment Planning.....	(2)
1.2.2 – Dose Calculation Methods .....	(3)
1.2.2.1 – Introduction to Monte Carlo Based Dose Calculation Model.....	(3)
1.2.2.1.1 – Monte Carlo Particle Transport.....	(4)
1.2.2.1.2 – Photon Interactions .....	(5)
1.2.2.1.3 – Electron Transport.....	(6)
1.2.3 – Monaco Treatment Planning System .....	(7)
1.2.3.1 – Introduction to Monaco .....	(7)
1.2.3.2 – Dose Calculation Algorithms in Monaco.....	(8)
1.2.3.2.1 – Pencil Beam Dose Calculation Algorithm in Monaco .....	(8)
1.2.3.2.2 – Monte Carlo Based Dose Calculation Model in Monaco .....	(10)
1.2.3.3 – Optimization .....	(13)
1.2.4 – Statistical Uncertainty .....	(15)
1.2.5 – Voxel Size.....	(17)
1.3 - Radiation Therapy Treatment Delivery and Dose Measurement.....	(17)
1.3.1 – Radiation Dose Measurement.....	(17)
1.3.1.1 – Diode Based Detectors .....	(18)
1.3.1.2 – Mapcheck Dose Measurement Device .....	(19)
1.4 – Gamma Analysis Index .....	(23)

1.4.1 - Introduction to Intensity Modulated Radiation Therapy Quality Assurance (IMRT QA).....	(24)
1.4.2 - The Gamma Analysis Index.....	(25)
1.4.3 – SNC Machine .....	(26)
<b>Chapter 2 – Materials and Methods .....</b>	<b>(27)</b>
2.1 - Radiation Therapy Treatment Planning .....	(27)
2.2 - Radiation Therapy Treatment Delivery and Dose Measurement.....	(28)
2.3 - Gamma Analysis Index .....	(29)
<b>Chapter 3 – Results .....</b>	<b>(29)</b>
3.1 – 3% / 3 mm Gamma Analysis Index Results .....	(30)
3.2 – 2% / 2 mm Gamma Analysis Index Results .....	(32)
<b>Chapter 4 – Discussion .....</b>	<b>(34)</b>
4.1 - 3% / 3 mm Gamma Analysis Index Discussion.....	(34)
4.2 - 2% / 2 mm Gamma Analysis Index Discussion.....	(35)
<b>Chapter 5 – Conclusion .....</b>	<b>(36)</b>
REFERENCES.....	(37)
ABSTRACT .....	(39)
AUTOBIOGRAPHICAL STATEMENT .....	(41)



## LIST OF FIGURES

Fig 1.1: Monaco Treatment Planning System Head and Neck Treatment Site [6].....	(3)
Fig 1.2: Comparison of 4 MeV electrons vs. 200 MeV electrons [5].....	(4)
Fig 1.3: Stages of Optimization Monaco [6]... ..	(13)
Fig 1.4: Mapcheck Grid Diode Spacing [19].....	(20)
Fig 1.5: Mapcheck Setup [19].....	(21)
Fig 1.6: Gamma Analysis Index Illustration [2] .....	(26)
Fig 1.7: Snapshot of SNC Machine [24].....	(27)
Fig 3.1: Average Passing Gamma Index (%) and Standard Deviations Data.....	(30)
Fig 3.2: 3%/3mm - Plot of Average Passing Gamma Index (%) vs. Voxel Size (mm).....	(30)
Fig 3.3: 3%/3mm - Plot of Average Passing Gamma Index (%) vs. Statistical Uncertainty (%) .....	(31)
Fig 3.4: 3%/3mm – Scatterplot of Average Passing Gamma Index (%) vs. Beam Number (#). (31)	
Fig 3.5: 3%/3mm – Plot of Average Passing Gamma Index (%) vs. Beam Number (#) .....	(32)
Fig 3.6: 2%/2mm - Plot of Average Passing Gamma Index (%) vs. Voxel Size (mm).....	(32)
Fig 3.7: 2%/2mm - Plot of Average Passing Gamma Index (%) vs. Statistical Uncertainty (%) .....	(33)
Fig 3.8: 2%/2mm – Scatterplot of Average Passing Gamma Index (%) vs. Beam Number (#). (33)	
Fig 3.9: 2%/2mm – Plot of Average Passing Gamma Index (%) vs. Beam Number (#) .....	(34)

## **Chapter 1 – Introduction**

### **1.1 - Higher Statistical Uncertainty with Small Pixel Sizes Gives Higher Gamma Pass Rates Research Project.**

Radiation therapy treatment planning systems are moving towards the routine clinical use of Monte Carlo based computation methods for calculating radiation dose. As compared to traditional methods that employ the use of developed algorithms, Monte Carlo has been shown to demonstrate the greatest accuracy in computing a dose distribution. However, Monte Carlo calculations trade-off accuracy at the expense of computational time, which is correlated to the user input values of statistical uncertainty and voxel spacing [1]. The input of a numerically inappropriate value for these two metrics, can lead to noise generation when verifying the quality assurance of a calculated plan by the accepted model of ‘gamma index analyses’ [2, 3]. This can potentially allow a plan that would normally fail plan verification to improperly pass the dose calculation criteria. For our research study, we have calculated 10 radiation oncology head and neck clinical treatment plans using Monaco Treatment Planning System which employs a Monte Carlo based dose calculation system. For each plan, we varied the statistical uncertainty input values from 5%, 3%, 1% and 0.25%. We also varied the voxel size input values at 1 mm increments from 3 mm, 2 mm and 1 mm. All of these calculated treatment plans were then administered on a clinical Elekta Versa Linear Accelerator and each plan was evaluated for clinical pass/fail criteria using 3%/3mm and 2%/2mm gamma index evaluation criteria.

## **1.2 - Radiation Therapy Treatment Planning**

### **1.2.1 - An Introduction to Radiation Therapy Treatment Planning**

Radiation oncology treatment planning begins with a patient medical imaging scan. The initial imaging scan allows internal 3D imaging of the axial, sagittal and coronal planes. In addition to imaging patient anatomy, the replication of a patient's setup for a radiation therapy treatment plan (simulation) will be an important part of the patient scan [4]. Radiation therapy treatment setup will include: patient position of anatomical placement and the creation and use of accessory treatment equipment. Although simulation may involve magnetic resonance imaging (MRI), positron emission tomography (PET) and computer tomography (CT) imaging modalities, CT is by far the most widely used imaging modality for radiation therapy simulation. Once an imaging scan in simulation is performed, the physician is then able within a virtual simulation station to select the target isocenter. The isocenter location is then transferred to reference coordinates on a laser localization system which can then be marked directly on the patient. The patient is then able to leave, and the imaging scans are transferred over to a treatment planning system (TPS). While in the treatment planning system, the tumor, target volumes, and structures of interest are then localized and contoured within the selected software. Depending on user preference, there are two commonly used planning techniques: inverse treatment planning and forward treatment planning. In forward planning, the user inputs the number of radiation beams and information regarding each beam parameter including beam-modifying devices. When finished, the plan is optimized and the computer calculates the finished dose distribution [5]. Forward treatment planning is used more frequently on standard 3DCRT radiation therapy treatments. Inverse planning, which is used for intensity modulated radiation therapy (IMRT), begins with the user pre-determining what the desired dose constraints are going to be. The planner inputs the desired dose limits for the tumor volume and critical

structures. The treatment planning system then modulates the intensity of the beams in order to optimize the dose distribution to hopefully replicate the user desired constraints [6].

Once all particulars of the treatment plan have been finalized, the plan is now ready to reach the stages of calculating the radiation dose distribution of the plan.

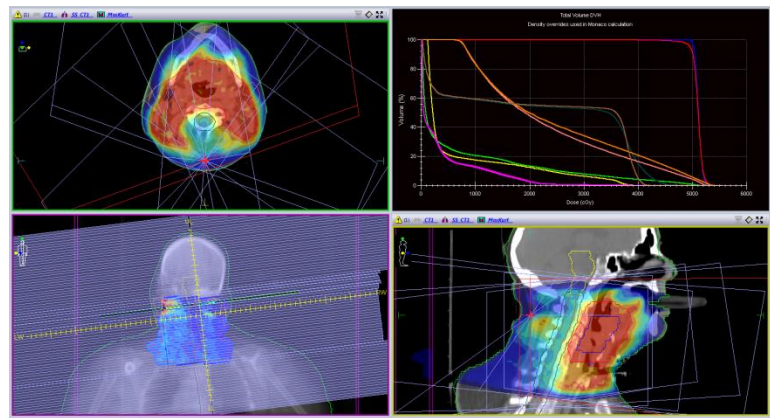


*Fig. 1.1: Monaco Treatment Planning System Head and Neck Treatment Site*  
From IMPAC Medical Systems, Inc, *Monaco® Training Guide*, 1st Vr. (Elekta Medical Systems, 2013).

## 1.2.2 – Dose Calculation Methods

When the specifications of the radiation therapy treatment plan have been finalized, the radiation dose distribution of the plan must now be calculated. Dose distributions calculated on a 3D anatomical image set, allow the user to observe the amount of radiation administered to each anatomical structure.

### 1.2.2.1 - Introduction to Monte Carlo Based Dose Calculation Model

The main concern with MC calculations when compared to algorithmic methods is the long treatment plan calculation times. To alleviate this problem, there have been a steady flow of research publications dedicated to accelerating the MC dose calculation in order to motivate routine clinical use [9]. It is fair to assume that in the near future, the MC dose calculation

methods will overtake algorithmic calculations as the customary way to calculate dose in radiation therapy treatment plans [10].

Using photon and electron transport physics, it is possible to consider the trajectories of individual particles and therefore the energy deposition due to each. The transport of an incident particle, and of particles that it subsequently sets in motion, are referred to as a particle history. Each history is uniquely determined by random selection from the probability distributions that control each interaction. A dose distribution can be built by summing the energy deposition in each particle history. However, a very large number of histories are required before the uncertainty in the distribution is small enough for it to be used in treatment planning.

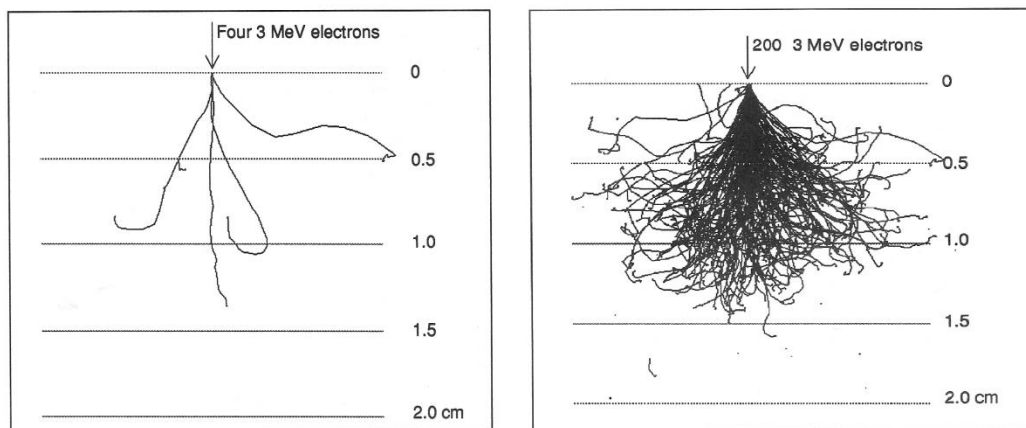


*Fig 1.2: Comparison of 4 MeV electrons vs. 200 MeV electrons.*

From P. E. Metcalfe, T. Kron and P. Hoban, *The Physics of Radiotherapy X-rays from Linear Accelerators*, 3rd Ed. (Medical Physics Publishing, 2007).

It is important to remember that the Monaco commercial TPS does have some approximations as compared to full MC codes used for research purposes.

### **1.2.2.1.1 – Monte Carlo Particle Transport**

The history of a particle is determined from:

- 1) the medium geometry and composition (user defined)

- 2) the initial state of the particle, such as position, angle and energy
- 3) the random selection from the set of probability distributions governing the possible interactions.

Within a history, the position, direction and energy are stored on a stack of variables. The term step is defined as the transport of a particle to its next position. The variables are updated with each step [5].

The considerations for variables to be updated with each step are:

- 1) Distance to the next interaction – the probability of selecting a distance is determined by the mean free path.
- 2) The type of interaction – whether the interaction is photoelectric, Compton or pair production.
- 3) The new angle and energy – the new angle and energy with each step will be determined from cross section tables.
- 4) If there are new particles – from these interactions new particles may be created.

#### **1.2.2.1.2 – Photon Interactions**

The most important interactions that take place are: Compton interaction, photoelectric effect, and pair production.

Compton interaction: is when a photon  $h\nu$  collides with an electron, transferring some of its energy  $E_{tr}$  to the electron. The photon is scattered and retains an energy of  $h\nu - E_{tr}$ . The energy transferred, photon scattering angle, and initial direction of the recoil electron are determined from the Klein-Nishina cross section data [5].

The Photoelectric effect: is when an incident photon loses its energy and ejects a bound electron. The energy left over from that required to free the electron is given to the electron as kinetic energy.

Pair production: is when an initial photon has an energy greater than the rest mass of an electron and a positron (1.022 MeV). The electron positron pair are created in a conversion of energy to mass, and the positron annihilates with an electron, producing a pair of 0.511 MeV photons.

### **1.2.2.1.3– Electron Transport**

While the distribution of energy imparted by photon interactions largely determines the dose distribution, electron transport is responsible for most of the computing time. At high energies, there could be many short electron transport steps corresponding to each photon step. For example, a 5 MeV photon undergoing a Compton interaction may set in motion a 3 MeV electron that may undergo many steps before running out of energy. The energy loss and multiple scattering interactions of an electron can be condensed where, after each step the electron is assumed to have lost a small amount of its energy via collision and radiative losses. The energy lost in each step is the product of the stopping power of the medium (dependent on the electron energy) and the length of each step. The angle of deflection after each step may be obtained by sampling from an angular distribution characterized by the scattering power and step length. Energy losses can often be grouped together and considered to be deposited evenly or continuously in each step. This is considered continuous energy loss and can be used by a continuous slowing down approximation (CSDA) [5].

A caveat to the CSDA method is that the randomness of individual electron motion is eliminated, which is not a 100% accurate depiction of electron transportation. In reality, a mixed approach is used where a user threshold is defined, in which above the threshold the electrons are

considered individually similarly to photons but, below the threshold the CSDA approach is used [5].

### **1.2.3 – Monaco Treatment Planning System**

Monaco is the marketed treatment planning software produced by Elekta Medical Systems. Elekta was founded in 1972 by Lars Leksell in Sweden and is headquartered out of Stockholm. Elekta was initially created for the production of two commercial products: The Leksell Stereotactic System and the Leksell Gamma Knife. Through great success, the company has acquired many other large successful radiation oncology industry companies such as: Phillips Medical Systems, Nucletron, CMS and IMPAC. With a more diverse production capability, Elekta, now produces a wide range of radiation therapy oriented products including: the Leksell Gamma Knife, Oncology software (Mosaik), Brachytherapy machines, linear accelerators, and treatment planning software (Monaco TPS) [12].

#### **1.2.3.1 – Introduction to Monaco**

Monaco is a treatment planning system that is designed to accommodate all major modalities of treatment that can be used in modern times. Monaco supports, 3D conformal radiation therapy, IMRT, VMAT, stereotactic MLC and cones.

Monaco is a well-established user-friendly treatment planning system with a broad suite of planning tools and bug free environment. Monaco has a vendor neutral planning platform which can accommodate all major linear accelerators. Monaco can also connect to any record and verify information system [13].



For 3D conformal treatment planning, Monaco uses a Graphics Processing Unit (GPU) for a collapsed-cone algorithm for the dose calculation. Monaco supports a range of modalities to cater to the clinic's needs including the support of wedges, boluses and VMC++ Electron Monte Carlo [13].

For intensity modulated radiation therapy (IMRT), which is the primary treatment method for radiation therapy. Monaco integrates the innovative biological cost functions with multi-criterial constrained optimization. Monaco also employs the use of a powerful leaf sequence optimizer. Monaco uses a robust Monte Carlo dose calculation algorithm to calculate the treatment plan dose distributions.

For volumetric modulated arc therapy (VMAT), Monaco can optimize single or multiple non-coplanar arcs simultaneously. Monaco offers the XVMC Monte Carlo dose calculation engine for a continuous electron and photon arc dose calculation [14].

### **1.2.3.2 – Dose Calculation Algorithms in Monaco**

Within Monaco Treatment Planning System, there are two distinct phases within the plan optimization process. The first phase involves the use of a Pencil Beam algorithm to optimize the beamlet weights. The second phase consists of the segment weights being optimized by method of a Monte Carlo Algorithm [6].

#### **1.2.3.2.1 – Pencil Beam Dose Calculation Algorithm in Monaco**

The Finite Pencil Beam algorithm was modeled using Monte Carlo simulations. Inhomogeneities, depth dose and off axis factors are taken into account by the algorithm. The idea behind pencil beam algorithms is that you can represent large fields by summing many small pencil sized beams [6].

For a precise PB algorithm, it is important to include: i) penumbra parameters for various field sizes, ii) Depth dose curves for various field sizes, and iii) Off-axis depth dose curves.

The *2D dose distribution* of a PB of width  $(2x_0, 2y_0)$  is constructed as a product of two independent 1D profiles with equivalent weights [6]:

$$F(x, y, w, u_x, u_y, x_0, y_0) = w_1 f_x(x, u_{1x}, x_0) f_y(y, u_{1y}, y_0) + (1 - w_1) f_x(x, u_{2x}, x_0) f_y(y, u_{2y}, y_0)$$

$f(x, u_{2x}, x_0)$  models the primary penumbra.

$f(x, u_1, x_0)$  models off-axis head-scatter and phantom scatter distributions.

Parameters,  $u_{1x}, u_{2x}, u_{1y}, u_{2y}, w_1$  are dependent on the depth in phantom, field size and ssd.

During commissioning of the PB, the system generated the parameters  $u_1, u_2, w_1, w_2$  from fitting to MC calculated profiles at 90 cm SSD. They are stored in lookup tables for depths from 0 to 30 cm in 2-10 mm increments, and for fields like 4x4, 10x10, 20x20 cm<sup>2</sup>.

The full dose distribution by a beamlet is given by [6]:

$$D(\mathbf{r}) = F\left(\frac{x}{r_a}, \frac{y}{r_a}, w(d), u_x(d), u_y(d), x_0, y_0\right) * A(d_{rad}, \theta) * \left(\frac{1}{r_a}\right)^2$$

$A(d_{rad}, \theta)$  is a scaling factor dependent on the depth and offset of the beamlet from the CAX.

$d_{rad}$  is the radiological depth of the point  $r_a$  (when dealing with heterogeneities)

$\theta$  is the angle between CAX of the beam and beamlet.

$r_a$  is the length of vector  $r_a$  in units of source to isocenter distance.

$A$  is a value stored in tables as a function of depth and angle (like off-axis).

The dose is calculated with a four step process [6]:

- 1) Find the rescaling functions to adjust the shape of the pencil beam to account for changes in ranges and lateral spread of scatter electrons and photons. ‘Penumbra widening factors’ =  $f_{u1}(\rho)$  for  $u_1$  etc.
- 2) Find  $u_1(t), u_2(t), w_1(t), w_2(t)$  in the lookup tables obtained during the commissioning of the pencil beam in water.
- 3) Correct  $w_1, w_2$  by applying factors  $f_{u1}(\rho)$  to correct for steepness parameters.

## 4) Calculate dose.

In Monaco, each dose element has its own weight. For example, if a segment (or beamlet) has 4.5 MU, its weight is 0.045.

The total dose calculated by adding all the beamlets is [6]:

$$D = \sum_{i=1}^N w_i D_i$$

$D_i$  = is the dose distribution of beamlet  $i$ .

$w_i$  = is the weight.

### 1.2.3.2.2 – Monte Carlo Based Dose Calculation Model in Monaco

The Photon Monte Carlo algorithm uses a Virtual Source Model to decrease the calculation time. The dose calculation takes beam modifiers and tissue inhomogeneities into account.

The Monte Carlo method uses random numbers to simulate behavior seen in nature. The result is an average of multiple random contributions.

Within the Monte Carlo method: machine characteristics are reflected, treatment aids are modeled, patient properties are reflected, and particles are tracked from source to end [6]. The Monte Carlo method simulates a large number of particle histories until all particles are absorbed or have left the calculation volume. The amount of absorbed energy of each particle track in each voxel are calculated and stored. Statistical uncertainty of the dose distribution will be determined from the number of photon and electron histories. For XVMC, the system starts to track particles at the patient surface.

Simulating the fluence engine can be done many ways. One can simulate the entire photon production from the wave-guide, typically, using the BEAM package to do detailed head modeling and simulation. The photon production can also be simulated at a point downstream of

the produced particles. The assumption is that the particle production is reproducible within a certain level of uncertainty.

The linac fluence can either come from the phase-space data or from a virtual source model. The phase-space data looks at the particle position, energy and direction of each particle from the MC simulation of the machine head. This method is time consuming and requires a lot of storage data. The virtual source model allows each linac head component to be treated as a sub-source, being primary, secondary, and electron contamination. The parameters for the VSM are extracted from full space data simulated with MC code BEAMnrc. For an accurate source model, the input of incident beam data is required. The data comes from the phase-space data which describes position, energy and direction of each particle from a MC simulation of the machine head. You can extract the required information from the distribution functions, such as, the energy spectrum, the primary and the scattering fluence distributions. This is called Virtual Energy Source (VSF) [6].

The Virtual Source Model (VSM) is based on three virtual sources: The primary photon source located at the target position, the secondary photon source located at the base of the primary collimator and the electron contamination source located in the base of the flattening filter [6].

With respect to beam modifiers, it is possible to model the MLC by a transmission filter. It simulates all passive effects, including, rounded leaf tips and stepped leaf sides. When particles go through the jaws, total absorption is considered if jaw transmission  $< 1\%$ . Dose can be computed from the average dose from the contribution from each particle in the given voxel. Where  $k$  indicates the voxel and  $i$  indicates the photon [6].

$$D_k = \frac{1}{N} \sum_{i=1}^N d_{i,k}$$

The system computes the uncertainty as the difference from individual particle doses and average dose.

$$\sigma^2 = \frac{1}{N} \sum_{i=1}^N (d_{i,k} - D_k)^2$$

In order to simulate the photon transport, the first step is to sample the distance from a given interaction point to the next (mean free path). The mean free path can be sampled from inverting the travelling probability function  $P(s)$ .

If  $r = 0$ , then the particle path is zero. If  $r = 1$ , then the particle path will be infinity and the particle will go outside the volume or patient.  $\mu$  is the probability per path length of a particle interaction [6].

The system determines the interaction type by energy and atomic number of the absorbing material. The three dominant interaction types are: Photoelectric, Compton, and Pair Production.

Once, the particle interacts via one of these mechanisms, the next step is to determine the energy and direction of the secondary particles using the differential cross sections [6].

In order to reduce the duration of the Monte Carlo dose calculation method, the use of Variance Reduction Techniques (VRT) are applied. XVMC uses VRT, so, it is 15-20 times faster than EGS but has an accuracy to EGS within  $\sim 1\%$ . The VRT reduction techniques are listed as follows: History repetition, Photon Splitting, Russian Roulette and Truncation Methods [7].

Monaco's XVMC calculates dose based upon mass density (g/cc). Monaco first converts CT numbers to relative electron densities based on CT-to-ED files. Electron densities are then

converted to mass densities. Monaco then assigns interaction probabilities and stopping powers to each voxel based on its mass density [6].

### 1.2.3.3 - Optimization

The workflow for the optimization process can be summarized via chart as follows,

<u>Optimization Process</u>	
Stage 1:	1a) Beamlet Decomposition
	1b) PB Absolute Dose Calculation
	1c) PB Weight Optimization
	1d) Output
Stage 2:	2a) Fluence Segmentation
	2b) MC final absolute dose calculation
	2c) Segment Weight Optimization

*Fig 1.3: Stages of Optimization Monaco*

Stage one, of the optimization process applies the use of the pencil beam algorithm for the optimization of the beamlet weights.

1a) Beamlet Decomposition: For the dose calculation and optimization process, Monaco divides each beam into smaller beamlets. Within each beamlet, the width can be user defined but the length is pre-determined by the length of the multileaf collimators (MLCs) [6].

1b) PB Absolute Dose Calculation: The Pencil Beams are commissioned from the MC dose distributions normalized to 100MU during the modelling process. Therefore, the beamlet doses add up to a large field of 100 MU. The parameters from the fsPB kernel are determined from broad beam dose distributions computed with the XVMC Monte Carlo dose from a fitting procedure. The fsPB dose distributions are stored for various broad field sizes and depths. The beamlet dose distributions are stored in terms of fitting parameters and account for dose contribution of each beamlet to add up to a broad beam dose of 100MU. The relationship between MU and absolute dose is obtained at this point [6].

The total dose of the distribution,  $D_0$ , is the weighted sum of the individual dose distributions of the beamlets.

$$D_0 = \sum_{j=1}^n D_j \phi_{j0}$$

$$MU_{Beamlet\ j,0} = \phi_{j0} * 100$$

where,  $D_j$  = dose distribution of fluence element j.

$\phi_j$  = weight of fluence element j in the total fluence distribution.

1c) PB weight optimization: The weights,  $\phi_j$  of all individual pencil beams are varied simultaneously by an iterative algorithm to meet the prescription requirements. The optimizer uses knowledge of the location of anatomy structures. The dose from the collection of weighted beamlets to minimize a cost function is the sum of planning objectives. Each beamlet needs to be varied for the modulated dose distribution.

1d) Output: The outputs of stage 1 are the beam ideal modulated intensity maps (weighted fluence maps) and the modulated ideal dose distributions.

The second phase employs the use of the Monte Carlo Algorithm to optimize the segment weights.

2a) Fluence Segmentation: The goal of fluence segmentation is to transform the continuous profile into field segments that have no intensity modulation of their own. The static sequencer performs a number of operations on the fluence profiles in order to extract a number of field shapes. These field shapes are then turned into proper MLC shapes.

2b) Final Monte Carlo Absolute Dose Calculation: Once the segments have been created, the MC dose calculation begins. The model is calibrated according to the measured dose for the reference field size provided by the user.

Monaco delivers a pre-calculated number of particles for each segment based on a specified dose uncertainty. Monaco tracks the energy and will integrate the dose deposited in the voxel which is related to 100 MU according to the system calibration in the modelling process. The dose uncertainty of a Monte Carlo computation depends on the number of energy deposition events that occur in a scoring volume and the energy of the distribution of these events [6].

Monaco uses an empiric formula to link the voxel volume, the particle flux, and the dose uncertainty. The empiric formula allows Monaco to calculate the number of particles to be delivered and tracks the absorb dose per voxel. These segment dose distributions will be weighted by the segment weight calculated from the optimization process at stage 1b). The total dose is calculated by,

$$D = \sum_{i=1}^N w_i D_i$$

$D_i$  = the normalized dose distribution of segment  $i$ .

$W_i$  = the weight of segment  $i$ .

2c) Segment Weight Optimization: A final segment weight and segment shape optimization will be performed to calculate the final optimal segment distribution [6].

#### **1.2.4 – Statistical Uncertainty**

The objective of a Monte Carlo simulation is to produce a calculation of radiotherapy dose that is reproducible. In reproducibility, the reference is to have successive simulations with different particles that give almost identical results. This is particularly difficult because the position and magnitude of energy deposition events will be different each time. In order to do this we must limit statistical uncertainty in the calculations. The goal in Monte Carlo is to have



the average behavior of N particles to be the same as that of other N particles. Between dose prescription to a tumor and the actual dose delivery, a large number of steps are involved. During each step, a particular uncertainty is introduced, accumulating to an overall uncertainty for the full process of dose delivery [5].

The amount of energy deposited in a voxel is a stochastic variable obeying Poisson statistics. If the mean is denoted by  $\lambda$ , the variance can be calculated as  $\sigma^2 = \lambda$ . In successive simulations, and the standard deviation can be calculated by  $\sigma = \lambda^{\frac{1}{2}}$ .

The statistical uncertainty may be calculated by  $\frac{\sigma}{\lambda}$  and equals  $\frac{1}{\lambda^{\frac{1}{2}}}$ .

From this calculation, we can determine that the statistical uncertainty decreases with the square root of the total energy deposited. The statistical uncertainty will also decrease with the square root of the number of incident particles. Therefore, to halve the uncertainty, we must quadruple the incident particles and also quadruple the computation time. It is important to know the uncertainty, so that we are aware of the error in the calculation [5].

If we look at a sample of incident photons: 1000, 4000. As an example the uncertainty of 4000 photons will be halved from that with 1000.

Within Monaco treatment planning system, the user is given the option to calculate statistical uncertainty based on per control point or per plan.

For the research presented here, we have decided to calculate with respect to per plan. Calculating statistical uncertainty per plan is in reference to the statistical uncertainty that you are willing to accept for the final dose calculation [6].

### **1.2.5 – Voxel Size**

Voxel size in 3D or in 2D, is referred to as grid spacing refers to the uniform spacing of the calculation points on a grid. The volume calculation grid itself is defined by the contoured structures in which the user selects the voxel size within the contoured structure. If a structure is small, it is ideal to calculate the structure using a small grid size and likewise if the structure is big apply a large grid size. As the grid size gets smaller, the calculation time increases. It is also important to note that if the grid size is too large, that it can lead to poorer resolution and create a less accurate monitor unit calculation. As a good rule of thumb it is advantageous to have the grid slicing at least as small as or slightly smaller than the CT slice spacing [6].

## **1.3 – Radiation Therapy Treatment Delivery and Dose Measurement**

### **1.3.1 – Radiation Dose Measurement**

When the science of radiation oncology is discussed, the first topics that come to mind are often related to the specifics of treatment or cancerous pathology. One of the most complex, overlooked and essential sciences that must be mastered in order to correctly administer a radiation therapy treatment is the science of dose measurement. Modern day radiation treatment plans use complex treatment methods to deliver the most appropriate amount of radiation dose, while sparing nearby organs that may be at risk. Being able to accurately measure radiation dose to replicate the output from these complicated techniques is absolutely imperative if a patient is to be treated with radiation. Dose measurement devices are used in order to give security to the patient and health care administrator that the radiation dose planned is within a numerical tolerance to the radiation that is actually to be delivered as a treatment. More specifically, dose measurement devices are used for direct measurement, to perform routine quality assurance on imaging or treatment machinery, and to calibrate the equipment to an accurate standard. There

are many different kinds of dose measurement devices and different kinds of dose measurement techniques currently used within radiation physics. For this research project, a modern dose measurement device called Mapcheck was employed, which utilizes diodes as its primary dose detection method.

### **1.3.1.1 – Diode Based Detectors**

A diode is a “dose measurement device that produces a large electrical current when an external voltage is applied. The resulting flowing electrical current comes from electrons raised to an excited state initially caused by the event of an interaction taking place.” [15]. Diodes consist of semiconductor radiation conductors that are typically Silicon or Germanium. Chemical elements like Si and Ge are doped with impurities that produce p-type semiconductors and n-type semiconductors. N-type semiconductors are doped with electron donors (P, As, Se) and p-type semiconductors are doped with electron acceptors (Ga, In) [16].

A radiation sensitive diode is formed by a thin layer or one type of semiconductor on top of a substrate from the other type. The zone between the two materials is called a p-n junction and it is depleted of charged particles and is a barrier for current. When the semiconductor is irradiated, electrons and electron holes are set free and a current now flows.

Diode semiconductors can be operated in two different modes: with bias and without bias. With bias, the current is measured as a function of the bias using an ampere meter. Without bias, the voltage generated is proportional to the radiation intensity. The voltage leads to a current, and the charge collected from the diode can be taken as a measure of dose. For most radiation applications, the diode is used within this mode [15].

Diodes are extremely sensitive radiation detectors and can be constructed with very small volume and spatial resolution. A typical diode sensitive volume is approximately  $0.2 \text{ mm}^3$  and produces roughly 1 nano-coulomb of current for every 1 cGy. For beam scanning, a diode is often used as a replacement for an ionization chamber. Drawbacks of the diode detector include: loss in sensitivity with radiation damage, temperature sensitivity  $0.1\% / \text{C}^\circ$ , angular response, requirement of high density build up, dose rate dependence, and energy dependence at low energy [17, 18].

### **1.3.1.2 – Mapcheck Dose Measurement Device**

The dose measurement device of choice for my research project is a diode based device called Mapcheck. Mapcheck consists of 445 diode detectors and is designed to measure dose distributions resulting from an IMRT plan. Mapcheck is considered to be simple to use, basically you complete the treatment plan within the treatment planning software. Generate a QA plan within the treatment planning software on a flat homogenous phantom at a desired depth and replicate the depth on the Mapcheck dose measurement device. The treatment plan generated must be orthogonal to the gantry at the time of beam delivery (exception, add on device for non-zero gantry measurement). Mapcheck measures the planned dose measurement from the QA plan, the calculated plan files can be saved, and the accuracy of the two plans can be compared [19].

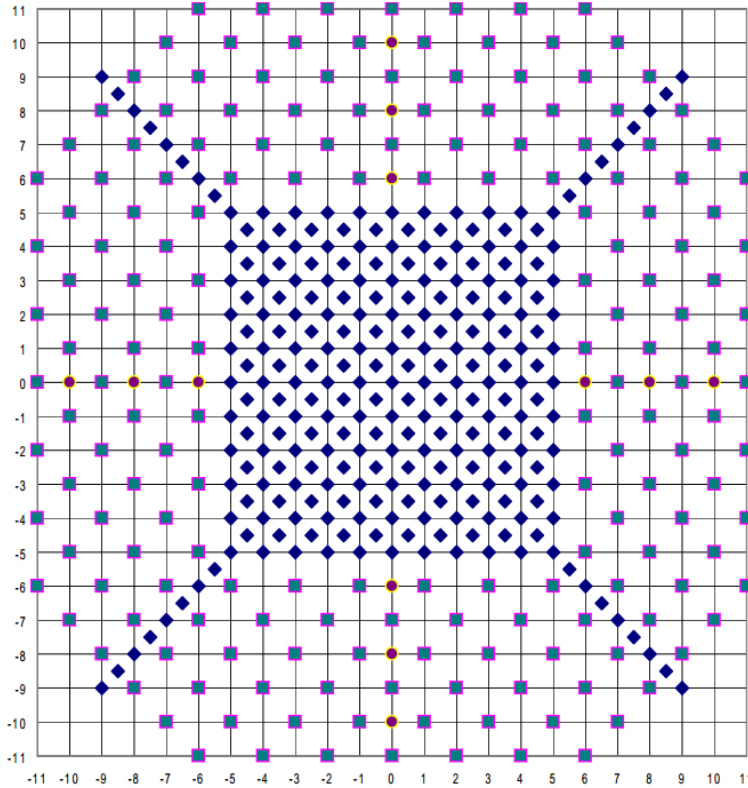


*Fig 1.4: Mapcheck Grid Diode Spacing*

From Mapcheck, *Mapcheck User's Guide*. (Sun Nuclear Corporation, 2006).

Mapcheck has 445 n-type radiation hardened, silicon diode detectors arranged within a 22 cm octagonal grid. The inside 10 x 10 cm region contains detectors that are 7 mm spacing apart. The outer region contains detectors that are 14 mm spacing apart. When a diode detector is exposed to radiation, the detector generates a charge that is proportional to the dose received at that point. Each charge value is integrated, converted from analog to digital, and sent to the computer. Two calibration factors are applied, which I will mention in brief detail, and the dose is displayed per diode. Also, there is an automatic background measurement made, as soon as the Mapcheck device is turned on.

Mapcheck has  $2.0 \pm 0.1 \text{ g/cm}^2$  inherent total buildup to the diode detector junctions which has a linear depth of  $1.35 \pm 0.1 \text{ cm}$ . Mapcheck is capable of measuring electrons within the energy of 6 MeV to 25 MeV and photons from 1.25 MeV (Co-60) to 25 MV. Mapcheck has

a dose limit of 330cGy and has light field alignment for 5x5cm, 10x10cm, 15x15cm, and 20x20cm. Mapcheck also exhibits little detector response variation from performing measurements at different time periods [19]. Mapcheck exhibits little measurement variation with time duration. A study was performed where two comparable measurements were taken, one at 1 hour from calibration and another 1 month later. The discrepancies between the two measurements were found to only be within 1% relative variation from each other [20].

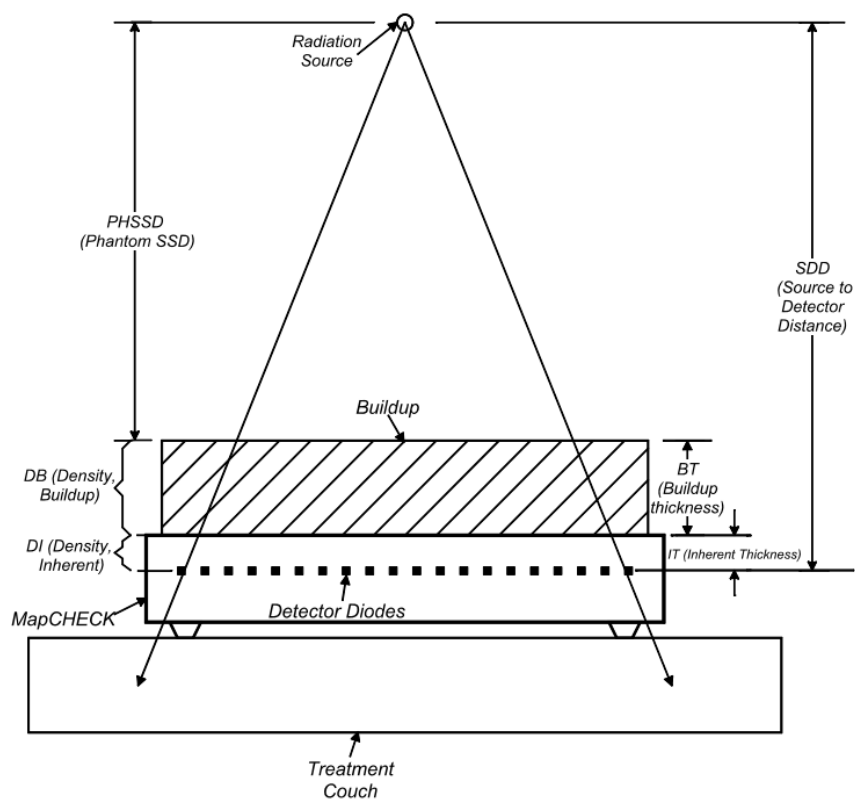


*Fig 1.5: Mapcheck Setup*

From Mapcheck, *Mapcheck User's Guide*. (Sun Nuclear Corporation, 2006).

There are two primary calibrations that must be performed for proper operation with Mapcheck: an array calibration and an absolute dose calibration. The array calibration is a process of determining the relative sensitivity differences between each of the detectors in the Mapcheck instrument. The differences are stored as individual correction factors to be applied to the raw measurements for each detector. This eliminates response differences between individual

detectors. The absolute dose calibration converts all the measured Mapcheck relative dose values to absolute dose values by applying a single calibration factor to all detectors [19].

There is also a background correction required prior to each measurement session, this accounts for the inherent cable and diode noise in the absence of radiation [17].

Although incorporating Mapcheck for daily use is considered an easy task, the complexity of radiation oncology does carry over a certain level of difficulty to the use of any dose measurement device. A common error that may occur is with regards to the understanding of how Mapcheck is used to perform IMRT QA for a patient radiation plan. The QA dose map is itself a recalculation, on a phantom, of the dose resulting from the beam fluence defined by the planning system and which is delivered on a linear accelerator. It's important to select an appropriate depth within the generated patient QA plan that can be tested on the Mapcheck device. An ideal amount of buildup for Mapcheck is from 0 to 5 cm. Incorporating a large amount of buildup depth creates scatter, which will damage the electronics. Buildup depth is also a common source of error when properly setting Mapcheck up to the same depth used within the QA plan generated. If this is a possible cause of error, the problem should become apparent when observing the measured to calculated dose profiles. Another common source of error is setting up Mapcheck off alignment with the linac cross-hair or having a device rotation. Anytime a network is used in tandem to many different software programs, there potentially could be problems in saving and acquiring the proper files for comparison. Proper operation of many different types of software is an obvious cause for increasing error. It is also possible that there could be a problem with the initial warm-up calibration or measured calculated calibrations being applied. The possible numerical error sources associated with the Mapcheck Calibration Error (MCE) are [19]:

- i) Array Calibration factor uncertainty ~ 0.006.
- ii) SDD difference between Mapcheck absolute calibration and standard chamber calibration ~0.004 for a 2mm difference at ~100cm SDD.
- iii) Accelerator fluctuation between Mapcheck absolute calibration and standard chamber calibration ~0.002.
- iv) Diode response variation due to temperature difference at calibration time and measurement time ~0.006 per degree °C.
- v) Overall Mapcheck Calibration Error (MCE) = 0.01 with a temperature change of 1°C.

It's recommended, that a few very simple plans are made and saved for quick access to allow the quick discovery of a potential problem. The plans may be standard 15x15, 10x10, 5x5 single fields calculated at 100 cGy. Bringing up these fields and measuring them with Mapcheck will allow a quick and easy detection to discover calibration problems.

Within TG 119, a report on IMRT commissioning, five institutions utilized Mapcheck diode detector for their measurement device over five different studies for individual field measurements. The average percentage of points passing the gamma criteria of 3%/3 mm over the test plans was 97.36% with an average standard deviation ( $\sigma$ ) of 1.66 [21]. This example demonstrates Mapcheck's accurate and steady measurement capability.

#### **1.4 – Gamma Analysis Index**

The commissioning of a three-dimensional treatment planning system requires the comparison of the measured and calculated dose distributions. There have been different techniques that were developed to facilitate quantitative comparisons, including superimposed isodose profiles, dose-difference, and distance to agreement (DTA) distributions. By far, the most commonly used method, the Gamma Analysis Index (GI), was first introduced by Low et.al [2, 3].



### **1.4.1 - Introduction to Intensity Modulated Radiation Therapy Quality Assurance (IMRT QA).**

Modern day radiation therapy treatment plans are far more complex than what would have been used twenty years ago. Radiation therapy plans were first developed to administer radiation in large general shapes collimated with static, stationary radiation beams. Today's radiation treatments employ dynamic movement in all axes of the delivered radiation. The gantry rotates while the MLCs constantly shape the radiation beam and in some delivered treatments the table is also moving at the same time. In order to parallel complex treatment delivery, treatment planning has come a long way with respect to advancing but also complicating the requirements to properly create a radiation treatment plan. Inverse planned IMRT treatments are known for producing very complex dose distributions with steep dose gradients between target volumes and critical structures. It's important to ensure that these complex dose distributions are first, calculated accurately and second, delivered with the same level of accuracy to the patient. In order to verify this, it is of common practice to perform patient specific QA as a means of plan verification. IMRT QA is required by Medicare billing guidelines and also for departmental American College of Radiology accreditation [22]. IMRT QA requires that each software created radiation therapy treatment plan be administered on a linear accelerator and measured for accuracy by means of a dose measurement device. The type of dose measurement device depends upon the form of treatment to be delivered but, for my research experiment, Mapcheck, a diode based detector was used. The 'Gamma Analysis Index' ( $\gamma$ ) was used as the quantitative method to compare the calculated dose distribution with the measured dose distribution [2, 3].

### 1.4.2 - The Gamma Analysis Index

Out of many different methods purposed to evaluate IMRT QA,  $\gamma$  is regarded as the most commonly used within the radiation oncology health care fields. The  $\gamma$  is used specifically for the comparison of two-dimensional dose comparisons. The treatment planning system dose calculation depth must be at the same depth as the measured dose distribution. For the user to utilize the Gamma Index they must enter an input value for distance to agreement (DTA) and percent dose difference. A commonly used percent dose difference and distance to agreement is 3%/3mm [21]. The  $\gamma$  formula requires both numerical input criteria to properly operate. If a Gamma Index value is calculated to be  $\leq 1$  the point has passed the acceptance criteria. A value  $> 1$  indicates a failing point. For a plan to be considered overall acceptable for the IMRT QA criteria, a plan must demonstrate greater than 90% of all points passing [2, 21]. The formula for the  $\gamma$  is listed as follows:

$$\gamma(r_m, r_c) = \sqrt{\frac{r^2(r_m, r_c)}{\Delta d_M^2} + \frac{\delta^2(r_m, r_c)}{\Delta D_M^2}}$$

In the formula,  $\Delta d_M$  denotes the distance to agreement that the user selected and  $\Delta D_M$  is the percent dose difference. The numerator  $r(r_m, r_c) = |r_c - r_m|$  is the absolute value squared of the difference in distance of the calculated and measured point.  $\delta(r_m, r_c) = D_c(r_c) - D_m(r_m)$  is the difference of the calculated dose and the measured dose. Lastly, it's important to note that all quality assurance formats used to compare the calculated and measured dose distribution have the capability to use the Gamma Analysis Index [2].

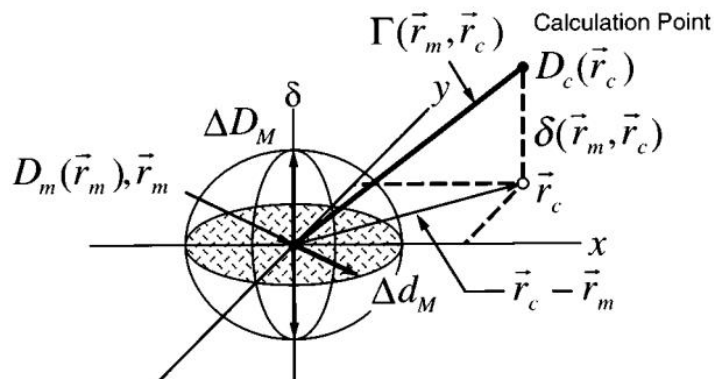


Fig 1.6: Gamma Analysis Index Illustration

From D. A. Low, W. B. Harms, S. Mutic and J. A. Purdy, Medical Physics **25** (5), (1998).

In a comprehensive study of three different planar IMRT QA techniques using Mapcheck, it was determined that for 10 clinical head and neck plans that the average passing rate for 1%/1mm was only 64.94 %. The average passing rates for 2%/2mm and 3%/3mm respectively were calculated as 91.86 % and 98.2 %. We have decided to calculate the GI for 3%/3mm and 2%/2mm and exclude 1%/1mm from our results due to the abnormally low percentage of passing points [23].

### 1.4.3 – SNC Machine

To apply the Gamma Analysis Index to the measured and calculated plans, we used the software SNC Machine, a product of Sun Nuclear Corporation. SNC Machine is a flexible software that can be used to calculate many different quality assurance tests. It is widespread, user friendly software that allows the user to select the file generated by the Mapcheck dose measurement device and compare it to the file exported from the treatment planning system calculated software [24]. The user can select to compare the dose distributions by just a distance to agreement or apply the full Gamma Index. The comparison can be performed in relative or absolute dose, and also requires an input value for threshold. A threshold is used to exclude low dose points from appearing to fail due to uncertainties. It is the percentage of normalization value

below which measurement points will be excluded from consideration for the pass-fail statistics. The result is a plot displaying the dose as a function of location axis for the compared measured and calculated dose distributions.

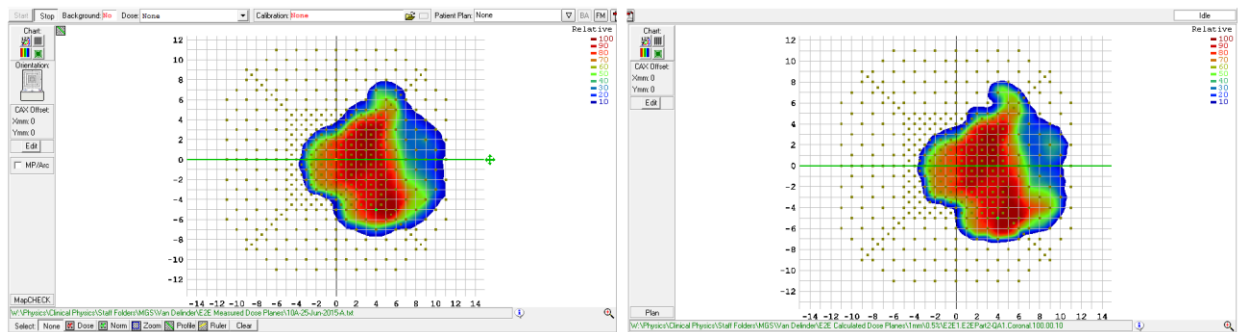


Fig 1.7: Snapshot of SNC Machine

## Chapter 2 – Materials and Methods

### 2.1 – Radiation Therapy Treatment Planning

For the research experiment, 10 clinical head and neck CT images and structure sets were brought over into Monaco from plans that were originally created within Eclipse. The 10 plans were created within Monaco as 8 IMRT fields, 6 MV energy, and prescribed to 60 Gy. 30 fractions of 200cGy per fraction were prescribed to achieve the total dose of 60 Gy.

The constraints for the 10 plans were motivated by RTOG 920 [25] and are listed as follows:

Max dose of 110%

95% of the volume gets 60 Gy

Parotid mean dose < 26 Gy

Brain Stem Max Point < 52 Gy

Spinal Cord Max Point < 46 Gy

100% isodose line covers the PTV

The dose calculation method for all of the treatment plans was the Monte Carlo method taken at a voxel size of 1mm and a statistical uncertainty of 1% calculated per plan.

Following the dose calculation for these 10 plans, the QA plans were made with the standard 30x30x30 Monaco phantom. The electron densities of the phantoms were forced to 1 in order to replicate the electron densities of water. The isocenter and point of interest were located at 5 cm deep. The dose calculation of the QA plans had their voxel sizes varied from 3mm, 2mm, and 1mm and also their statistical uncertainties varied from 5%, 3%, 1% and 0.5%.

## **2.2 – Radiation Therapy Treatment Delivery and Dose Measurement**

The first step to following through with delivering the QA plans on the linac is to make sure that all proper QA files are saved for access. By files, I am referring to all of the individual beams with varied voxel sizes of 3mm, 2mm, and 1mm and varied statistical uncertainties 5%, 3%, 1%, and 0.5%. These are all of the saved calculated plans that will be used for the Gamma Analysis index. The next step, is to send all of the QA plans to the Elekta Versa, for beam delivery and measurement. Due to the fact, that we are using Mapcheck for the dose measurement, all gantry angles were previously set to zero. This is because Mapcheck exhibits angle dependence and is only accurate for beam administration directly on the measurement device (gantry zero). With the plans exported properly to the Elekta Versa, the next important step is the actual setting up of the Mapcheck measurement device. Firstly, it's important to make sure that Mapcheck is properly balanced using the balance knob on the device. Also, before beginning, Mapcheck must be properly aligned with the crosshairs of the linac. The physical diode detectors are located 1.35 cm below the top surface of the Mapcheck. Also, Mapcheck has an inherent buildup distance of  $2.0 \text{ g/cm}^2$ . Due to this, caution should be used when setting up

Mapcheck. The 10 clinical plans were calculated at 5 cm depth. The technique to match this with Mapcheck is to set 100 SSD on the top of Mapcheck and then drop the table down to the detector diode marker. The reading should now be 98.65 cm on the ODI. To replicate 5cm deep, we now place 3 cm of solid water on top of the Mapcheck dose measurement device. Now, we can administer all the fields and save them accordingly for the Gamma Analysis Index.

### **2.3 – Gamma Analysis Index**

In order to compare the plan measured and calculated files, we used SNC Machine, product of Sun Nuclear and applied the  $\gamma$ . SNC is very easy to use and user friendly. Basically, you select the initial file that the  $\gamma$  will be calculated off of which is typically the measured plan. Then, you select the calculated plan and type in the % dose difference and distance to agreement (DTA). The option is given to select either relative dose or absorbed dose, for our study we used absorbed dose. Next, the  $\gamma$  button is clicked and compares all of the fields for all of the variations. Even though 3%/3mm is the clinically relevant  $\gamma$  analysis criteria used, we also gathered results for 2%/2mm.

## **Chapter 3 – Results**

The culmination of my results evaluating the effect of noise production on a Monte Carlo based dose calculation can be showcased in a few simple plots. For my experimental data, I have decided to evaluate the Gamma Analysis Index with both 3% dose difference/3mm distance to agreement (3%/3mm) and 2% dose difference/2mm distance to agreement (2%/2mm).

3%/3mm	1mm	2mm	3mm
5 %	99.60	98.99	97.66
3 %	99.56	98.96	97.63
1 %	99.14	98.78	97.94
0.5 %	98.91	98.84	98.05
2%/2mm			
5 %	98.80	95.22	90.55
3 %	98.76	95.24	90.55
1 %	97.77	95.75	93.26
0.5 %	97.02	96.00	94.15

Fig 3.1: Average Passing Gamma Index (%) and Standard Deviations Data

### 3.1 – 3% / 3 mm Gamma Analysis Index Results

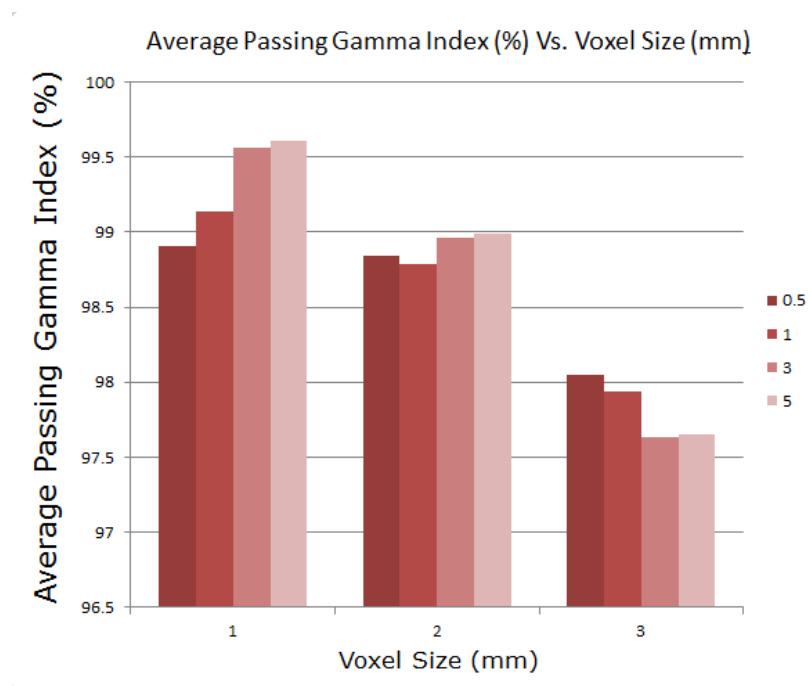


Fig 3.2: 3%/3mm - Plot of Average Passing Gamma Index (%) vs. Voxel Size (mm)

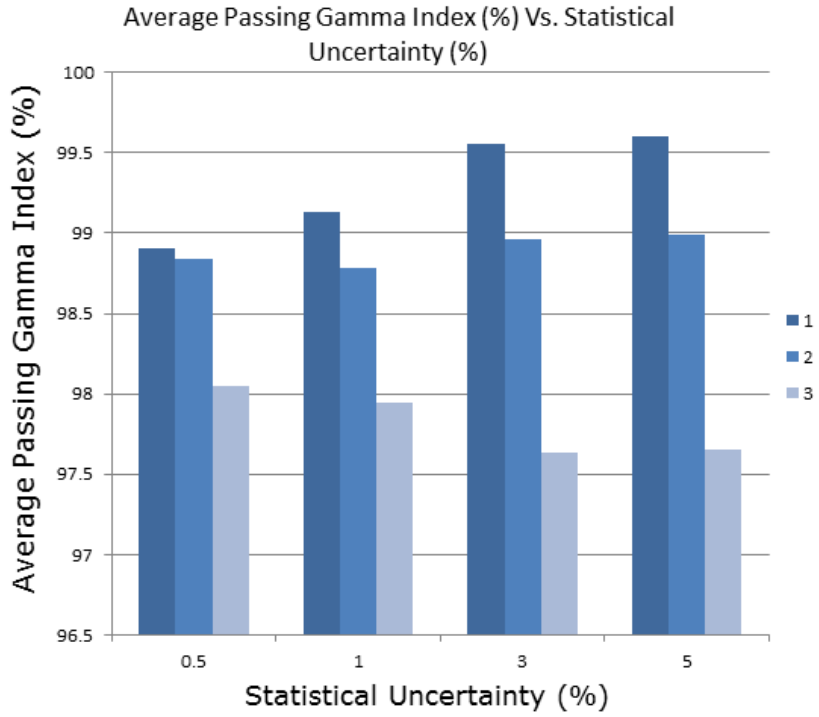


Fig 3.3: 3%/3mm - Plot of Average Passing Gamma Index (%) vs. Statistical Uncertainty (%)

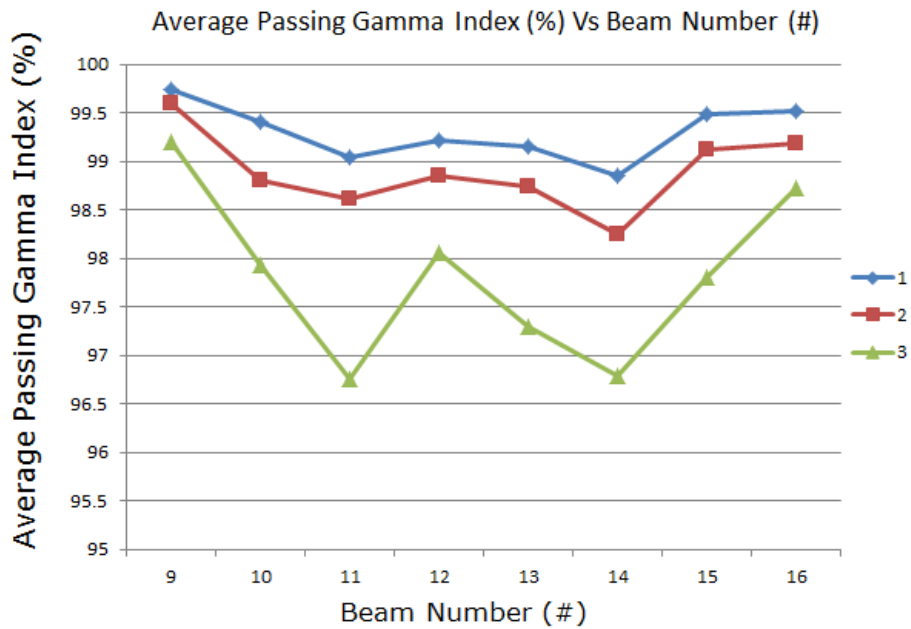


Fig 3.4: 3%/3mm – Scatterplot of Average Passing Gamma Index (%) vs. Beam Number (#)



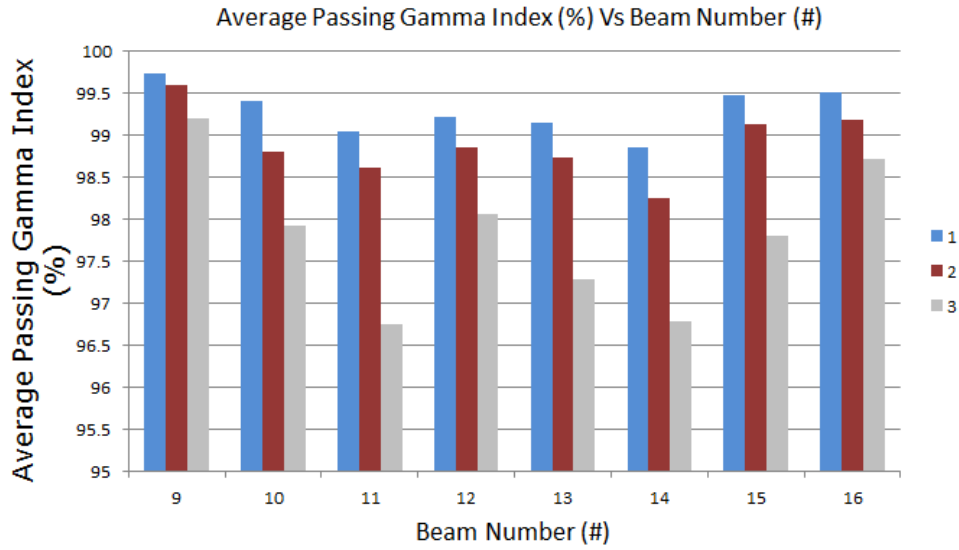


Fig 3.5: 3%/3mm – Plot of Average Passing Gamma Index (%) vs. Beam Number (#)

### 3.2 – 2% / 2 mm Gamma Analysis Index Results

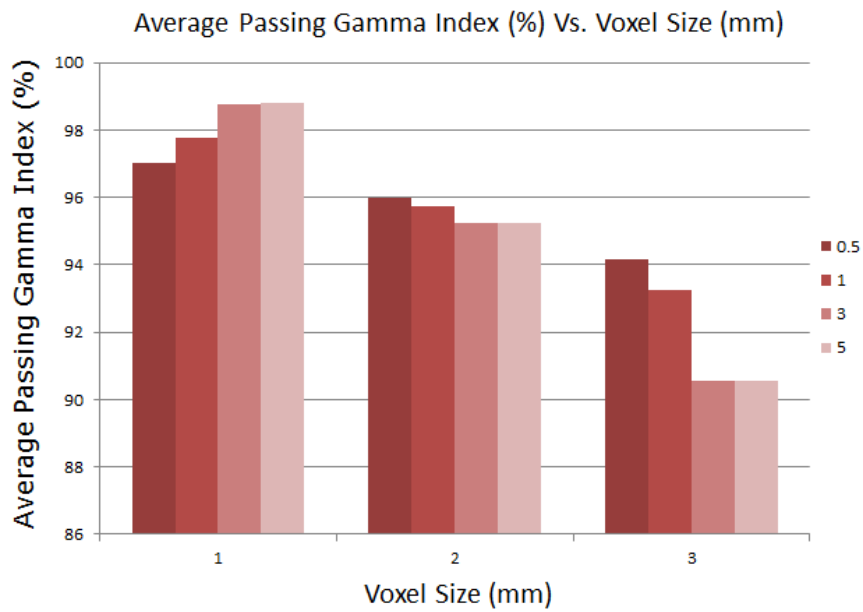


Fig 3.6: 2%/2mm - Plot of Average Passing Gamma Index (%) vs. Voxel Size (mm)

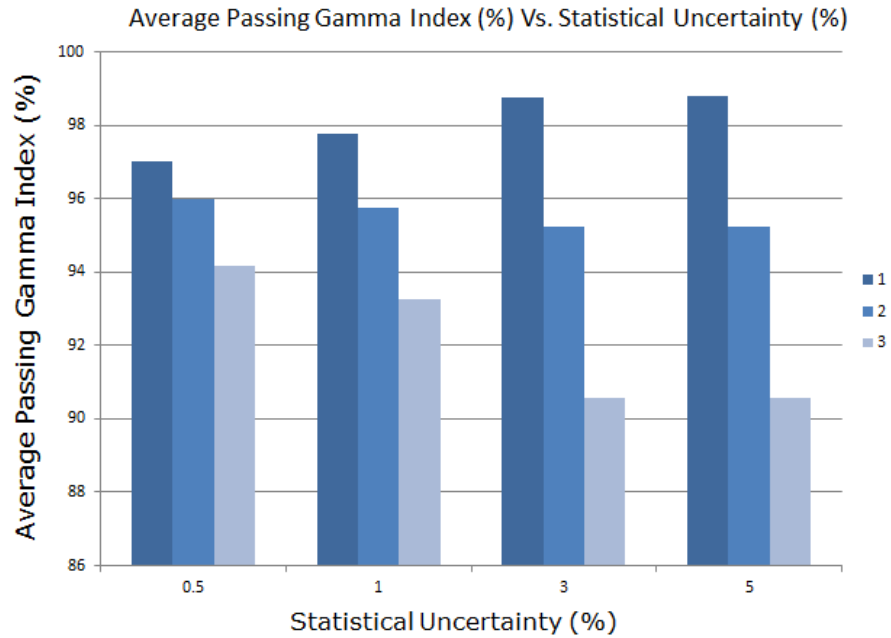


Fig 3.7: 2%/2mm - Plot of Average Passing Gamma Index (%) vs. Statistical Uncertainty (%)

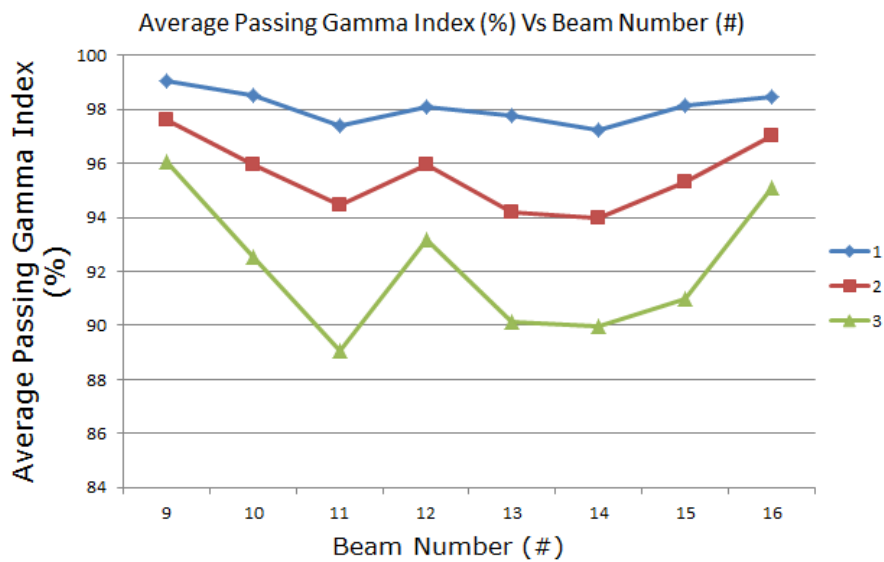


Fig 3.8: 2%/2mm – Scatterplot of Average Passing Gamma Index (%) vs. Beam Number (#)

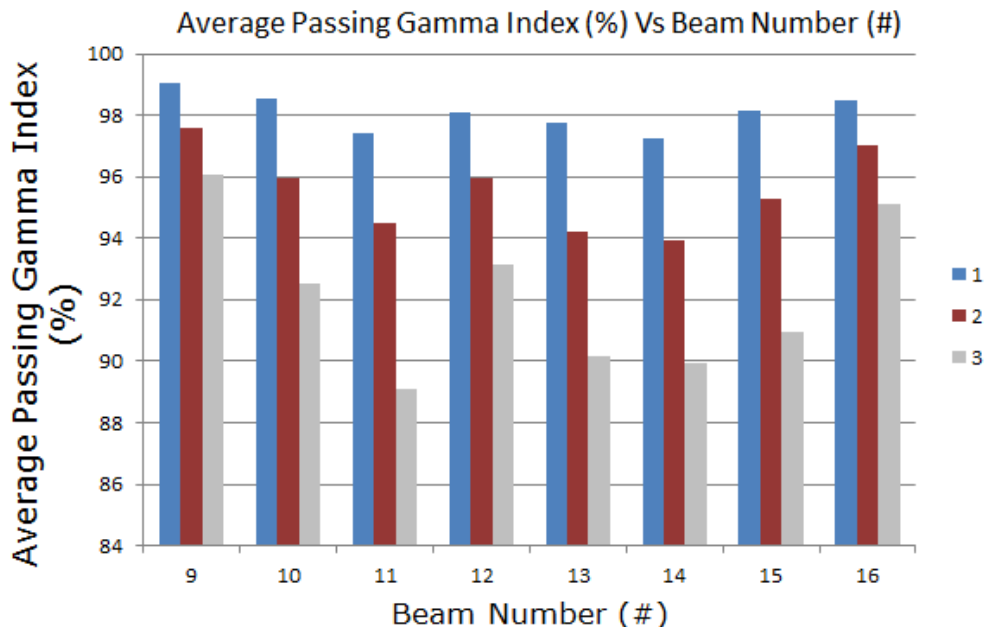


Fig 3.9: 2%/2mm – Plot of Average Passing Gamma Index (%) vs. Beam Number (#)

## Chapter 4 – Discussion

From a clinical standpoint, 3%/3mm is the common criteria but, there may be a few clinics that employ the use of 2%/2mm for their IMRT QA. Similarly, a few clinics may exist that utilize the calculated distribution as the selected reference distribution.

### 4.1 - 3% / 3 mm Gamma Analysis Index Discussion

For the 3%/3mm Gamma Analysis Index results, there are some interesting trends to mention from the plotted data. From plot 1 and also plot 2, it's easy to observe that there is an increasing average gamma pass percentage with decreasing voxel size. The reasoning for this is because, within the GI Analysis, we're picking a point in the measured dose profile and comparing to the calculated. As the calculated voxel size gets smaller, this allows for a greater amount of calculated points available to meet the criteria of the GI Analysis. Most importantly,

from the data displayed, there is clear evidence that at a small voxel size, (1mm) the increase in statistical uncertainty (noise) does increase the average gamma passing rate. In plots 3 and 4, there seems to be a low average gamma pass rate for beam numbers 11 and 14 at 3mm voxel size. At 2mm and 1mm voxel size, beam numbers 11 and 14 seem to even out with the rest of the fields.

#### **4.2 - 2% / 2 mm Gamma Analysis Index Discussion**

The results for the 2%/2mm Gamma Analysis Index showcase almost identical trends to the 3%/3mm. This is expected, with perhaps a few small variations due to the reasoning that the Gamma Index tolerances are significantly tighter. Comparing to 3%/3mm, we are seeing higher average gamma pass rates with smaller voxel size for the same reason mentioned above in the 3%/3mm. One interesting difference is that at the 2mm voxel size for 3%/3mm, the higher statistical uncertainties had higher average gamma pass rates than the lower statistical uncertainties. This is not the case for 2%/2mm. For 2%/2mm, 2mm voxel size the higher statistical uncertainties had lower average gamma pass rates.

The main difference between the 3%/3mm and 2%/2mm, is that because the tolerance is higher for the former, the average pass rates will be much higher. The 2%/2mm had some fields that were close to failing the acceptable plan verification amount being 90% of points passing. Also, there were more fields at the 3mm voxel size that had a significantly lower average gamma pass rate.

## Chapter 5 – Conclusion

For my research experiment, we looked at 10 clinical head and neck plans and varied the statistical uncertainty and voxel size to observe the effect noise had on passing Gamma Index Analysis rates. The results from the plans are conclusive; the average gamma index passing rate as a percent, does increase with increasing statistical uncertainty for small voxel size. Most specifically, this effect is observed when the dose distribution is calculated at a 1 mm voxel size. This is a confirmation of the sensitivity of the gamma index to noise first hinted in the publication entitled ‘Evaluation of the gamma dose distribution comparison method’ [3].

Monte Carlo based dose calculation methods have been proven to be more accurate than algorithmic methods. It would be fair to estimate that in the near future most treatment planning systems will employ the use of a Monte Carlo based calculation method to calculate the treatment plan dose. Input values of statistical uncertainty and voxel size will still be required by the user prior to the dose calculation. Caution must be given to the user when selecting the appropriate input values prior to calculation. As was concluded from this research experiment, a low voxel size 1mm and a high statistical uncertainty does increase the gamma pass rate percentage inaccurately. This could lead to an incorrect treatment plan that would normally fail to falsely-pass verification and be considered acceptable for patient treatment. The input value of statistical uncertainty is of critical concern because a reasonable value for the voxel size of the head and neck region is 1mm. A small voxel size calculated with the addition of a low statistical uncertainty can generate a very long calculation time for the complete dose distribution. Choosing the appropriate values for the voxel size and statistical uncertainty is an important part of the treatment planning process to be considered for an accurate treatment plan dose calculation.

## REFERENCES

1. P. Keall, J. Siebers, R. Jeraj and R. Mohan, *Medical Physics* **27** (3), 478-484 (2000).
2. D. A. Low, W. B. Harms, S. Mutic and J. A. Purdy, *Medical Physics* **25** (5), 656-661 (1998).
3. D. A. Low and J. F. Dempsey, *Medical Physics* **30** (9), 2455-2464 (2003).
4. C. M. Washington and D. T. Leaver, *Principles and Practice of Radiation Therapy*, 3<sup>rd</sup> Ed. (Elsevier Health Sciences, 2015), pp. 158-180.
5. P. E. Metcalfe, T. Kron and P. Hoban, *The Physics of Radiotherapy X-rays from Linear Accelerators*, 3<sup>rd</sup> Ed. (Medical Physics Publishing, 2007), pp. 325-330, 398-405, 408-412, 418-428, 430-431
6. IMPAC Medical Systems. Inc, *Monaco ® Training Guide*, 1st Vr. (Elekta Medical Systems, 2013), S. 819-855, 903-931, 931-977,
7. R. Popple and J.E. Cygler, *Monte Carlo Treatment Planning: Implementation of Clinical Systems*, Ottawa Hospital Regional Center (Unpublished).
8. I. J. Chetty et al., *Medical Physics*. **34** (12), 4818-4853 (2007).
9. N. Reynaert et al., *Radiation Physics and Chemistry* **76** (4), 643-686 (2007).
10. J. DeMarco, I. Chetty and T. Solberg, *Medical Dosimetry* **27** (1), 43-50 (2002).
11. I. Fotina et al., *Radiotherapy and Oncology*. **93** (3), 645-653 (2009)
12. G. G. Marcial, *Why Elekta May be A Stockholm Standout*. (BusinessWeek, 2009).
13. Elekta, *Versa HD Brochure*. (Elekta Medical Systems, 2013).
14. Elekta, *Physics 1: Medical Accelerator Introduction*. (Elekta Medical Systems, 2014).
15. J. T. Bushberg and J. M. Boone, *The Essential Physics of Medical Imaging*. (Lippincott Williams & Wilkins, 2011), pp. 633-634.
16. J.-C. Rosenwald and P. Mayles, *Handbook of Radiotherapy Physics Theory and Practice*, 1st Ed. (CRC Press, 2007), pp. 314-319
17. D. Létourneau *et al.*, *Radiotherapy and Oncology*. **70** (2), 199-206 (2004).

18. J. W. Burmeister, *ROC7040 Dosimetry Coursepack*. (Wayne State University, 2015), pp. 170-173.
19. Mapcheck, *Mapcheck User's Guide*. (Sun Nuclear Corporation, 2006), pp. S. 13-18, 21-22, 117, 120-123, 128-130, 132.
20. J. G. Li, G. Yan and C. Liu, *Journal of Applied Clinical Medical Physics*. **10** (2) (2009).
21. G. A. Ezzell *et al.*, *Medical Physics*. **36** (11), 5359-5373 (2009).
22. A. C. Hartford *et al.*, *American Journal of Clinical Oncology*. **35** (6), 612-617 (2012).
23. V. P. Keeling, S. Ahmad and H. Jin, *Journal of Applied Clinical Medical Physics*. **14** (6) (2013).
24. SNC Machine, *Automate Your QA*. (Sun Nuclear Corporation, 2015).
25. M. Machtay, *Radiation Therapy Oncology Group RTOG*, **0920** (2009).
26. J. Y. Huang *et al.*, *Journal of Applied Clinical Medical Physics*. **15** (4), 4690 (2014).

**ABSTRACT****HIGHER STATISTICAL UNCERTAINTY WITH SMALL PIXEL SIZES  
GIVES HIGHER GAMMA PASS RATES**

by

**KURT VAN DELINDER****December 2016****Advisor:** Dr. Michael Snyder**Major:** Medical Physics**Degree:** Master of Science

Monte Carlo (MC) based dose calculation methods trade-off accuracy at the expense of computational time, which is, correlated to the user input values of statistical uncertainty and pixel spacing <sup>(1)</sup>. It was first hinted by low et. al. that noise generated within either the calculated or measured plan distributions can affect the result of the plan verification by method of ‘Gamma Index Analysis’(GI) <sup>(2)</sup>. The purpose of this research experiment is to investigate a possible correlation between added noise from increasing MC statistical uncertainty and increasing the odds of a plan passing the GI verification criteria. For this research experiment, we calculated 10 head and neck radiation therapy treatment plans using the MC dose calculation method within Monaco TPS. We varied the statistical uncertainty values from 5%, 3%, 1% and 0.25% and varied the voxel size values from 3mm, 2mm and 1mm. The treatment plans were then administered on an Elekta Versa linear accelerator and measured using Mapcheck dose measurement device. Each plan was evaluated for clinical pass/fail using the GI Analysis with criteria 3%/3mm and 2%/2mm. For 1 mm voxel size, 3%/3mm GI, there was an increase in average gamma pass rates from 98.91% calculated at 0.5% statistical uncertainty to 99.61%



calculated at 5% statistical uncertainty. For 1 mm voxel size, 2%/2mm GI, there was an increase in average gamma pass rates from 97.02% calculated at 0.5% statistical uncertainty to 98.80% calculated at 5% statistical uncertainty. At 2 mm and 3 mm voxel sizes, there was not a clear demonstrable increase in average gamma pass rates. The experimental results conclude that the user must be careful when selecting a statistical uncertainty prior to performing a MC dose calculation. The input of a high statistical uncertainty does not lead to more points failing the GI, but paradoxically, can increase the chances that the evaluated radiation therapy plan will pass the acceptance evaluation.

## AUTOBIOGRAPHICAL STATEMENT

Born in Windsor, Ontario, Canada in 1986, Kurt has always had a fond interest in both the physical sciences and health care sciences. As a late teenager, he studied and found role models in the great innovative works of Thomas Edison, Henry Ford and Nikola Tesla. Inspired by their innovative footsteps, Kurt too wanted a niche where he could be given the opportunity to invent and develop new technologies that would also make a significant impact on society. Health care seemed to be the ideal science for such a feat to be achievable. To be even more specific, diagnostic health care. While looking more into this form of technology, it didn't take long for him to realize that he did not have the scientific background or ability to truly understand the workings of how these types of equipment are designed. They require not only a strong understanding in science and newly innovated technology but, also require a great deal of knowledge in computer software and a strong command of mathematical physics. Within a short period of time, Kurt found his path in life and future field in which he would pursue as a professional career, the field of Medical Physics.

In 2006, Kurt then came up with an academic plan. He would enroll in a B.Sc program in Radiation Therapy, get a M.Sc in Physics and then hopefully get accepted into Medical Physics and complete a Ph.D.

In the fall of 2007, Kurt first started the program Radiation Therapy at Wayne State University. Throughout the four year program, Kurt received high honours and graduated top of his class as summa cum laude. During the program, Kurt was also recognized and placed on the deans honour list for his superb grade point average of 3.72.

In the fall of 2012, Kurt began what would be his first Master of Science program within the field of general physics also at Wayne State University. Two years later, a completion of the class coursework was finished and also demonstrated the success of his thesis defense and acceptance of his written submission.

In the early months of spring 2014, Kurt received his acceptance letter from the University of Wayne State, Department of Medicine that he was accepted for fall enrollment into the medical physics graduate program. Two years later, and the completion of the Master of Science in Medical Physics course work, Kurt is currently preparing for the Ph. D. Qualifying exams for fall enrollment into the Medical Physics Ph.D. graduate program.